Families of periodic orbits for solar sails in the CRBTP

Patricia Verrier[1] and Thomas Waters[2]
University of Portsmouth, Portsmouth, Hampshire, PO1 3HF, UK

and
Jan Sieber[3]
University of Exeter, Exeter, EX4 4QF, UK

We use the numerical continuation package AUTO to investigate families of periodic orbits in the solar sail circular restricted three-body problem. For a sail orientated perpendicular to the Sun-line we find significant differences to the classical case for some families near the Earth, including the L_1 Halo family and retrograde satellite family. Specifically, we expand on existing results and find that the change in the Halo family H1 is associated with a bifurcation of a branch point in the retrograde satellite family, which splits H1 in half. We also track regions of stability within the family, and find some large amplitude stable orbits. For a sail tilted relative to the Earth-Sun line only we find large amplitude families with some stable orbits. Interestingly there is also a small range of parameters for which L_1 bifurcates into three separate points in this system.

I. Introduction

FAMILIES of periodic orbits are well known in the context of the circular restricted three-body problem (CRTBP) and have found numerous applications to space craft trajectory design. In this work we consider a modified CRTBP that includes radiation pressure, so that it is applicable to solar sails. We use the simple model of radiation pressure acceleration given by [1] for a perfect sail. This model uses the sail's lightness number β and normal vector $\boldsymbol{n}$ to parameterize the problem.

The classical CRTBP is conservative and as a consequence it is well known that periodic orbits form one-parameter families in the energy level for a given mass ratio. The solar sail CRTBP is only conservative if the sail's normal vector $\boldsymbol{n}$ is directed radially along the Sun-line. For a generic choice of $\boldsymbol{n}$ the system is non-conservative, and families can only be formed in β and the angles used to define the sail orientation. However,

[1] Research Associate, Department of Mathematics, University of Portsmouth, Lion Gate Building, Lion Terrace, Portsmouth, Hampshire, PO1 3HF, UK.
[2] Senior Lecturer, Department of Mathematics, University of Portsmouth, Lion Gate Building, Lion Terrace, Portsmouth, Hampshire, PO1 3HF, UK.
[3] Lecturer, College of Engineering, Mathematics and Physical Sciences, University of Exeter, Exeter, EX4 4QF, UK.

M. Macdonald (ed.), *Advances in Solar Sailing*, Springer Praxis Books,
DOI: 10.1007/978-3-642-34907-2_52, © Springer-Verlag Berlin Heidelberg 2014

there are some specific sail orientations that result in a non-conservative but reversible system, in which time reversible periodic orbits will also form one-parameter families [2, 3].

Numerical continuation methods provide a powerful tool for investigating such families of periodic orbits. For example, [4] demonstrate how the AUTO package [5] can be used to study elementary families emanating from the Lagrangian points in the classical CRTBP. Here one-parameter families can be continued by introducing artificial dissipation controlled by an unfolding parameter which will be zero for periodic solutions [6, 7, 8, 9].

Using AUTO we investigate families of periodic orbits for two specific choices of the solar sail orientation. The first case is the conservative system with the sail orientated perpendicular to the Sun-line. The second is the non-conservative but reversible system with the sail tilted relative to the Earth-Sun line. The following two sections describe the mathematical model and numerical continuation methods for generating the periodic orbits. The results for the two different sail angles are then presented and finally conclusions are given.

II. The Solar Sail CRTBP

We consider the motion of a solar sail in the context of the Earth-Sun CRTBP i.e. the Sun is the primary mass m_1, the Earth the secondary mass m_2 and the sail the massless test particle. In the rotating reference frame the Sun is located at $(-\mu,0,0)^T$ and the Earth at $(1-\mu,0,0)^T$, where $\mu = \frac{m_2}{m_1+m_2} = 3 \times 10^{-6}$ is the mass ratio. Units are used such that the distance between the Sun and the Earth, their angular velocity in the non-rotating frame and $G(m_1+m_2)$ are all unity, where G is the gravitational constant. The sail is located at $\boldsymbol{r} = (x, y, z)^T$ in this frame and is assumed to have a fixed orientation defined by its normal vector $\boldsymbol{n}$. The sail's position relative the Sun and Earth are

$$\boldsymbol{r}_1 = (x + \mu, y, z)^T,$$

$$\boldsymbol{r}_2 = (x - 1 + \mu, y, z)^T$$

respectively, as shown in Fig. 1. Following [1] the additional acceleration on a perfectly reflecting solar sail in this system is

$$\boldsymbol{a} = \beta \frac{(1-\mu)}{r_1^2} (\hat{\boldsymbol{r}}_1 \cdot \boldsymbol{n})^2 \boldsymbol{n}$$

where $\hat{\boldsymbol{r}}_1$ is the unit vector in the direction of $\boldsymbol{r}_1$ and $r_1 = |\boldsymbol{r}_1|$. The first case we consider has the sail orientated along the Sun-line so the acceleration is in the radial direction only i.e. $\boldsymbol{n} = \hat{\boldsymbol{r}}_1$. This system is conservative and Hamiltonian, and has equations of motion given by

$$\ddot{\boldsymbol{r}} + 2\boldsymbol{\omega} \times \dot{\boldsymbol{r}} = \nabla V$$

where a dot indicates differentiation with respect to time, $\boldsymbol{\omega} = (0,0,1)^T$ and the potential V is

$$V = \frac{(1-\mu)(1-\beta)}{r_1} + \frac{\mu}{r_2} + \frac{1}{2}|\boldsymbol{\omega} \times \boldsymbol{r}|^2$$

where $r_2 = |\boldsymbol{r_2}|$.

The second case we consider has the sail orientated at a constant angle γ to the Sun-Earth line i.e. $\boldsymbol{n} = (\cos\gamma\,, 0, \sin\gamma)^T$. The equations of motion in this case are

$$\ddot{\boldsymbol{r}} + 2\boldsymbol{\omega} \times \dot{\boldsymbol{r}} = \nabla U + \boldsymbol{a}$$

where the potential U is now

$$U = \frac{(1-\mu)}{r_1} + \frac{\mu}{r_2} + \frac{1}{2}|\boldsymbol{\omega} \times \boldsymbol{r}|^2.$$

This system is no longer Hamiltonian but remains reversible as the equations of motion are invariant under $(x, y, z, \dot{x}, \dot{y}, \dot{z}, t) \rightarrow (x, -y, z, -\dot{x}, \dot{y}, -\dot{z}, -t)$. Both systems are known to possess one-parameter families of orbits emanating from the equilibria equivalent to the Lagrangian points [10, 11, 12].

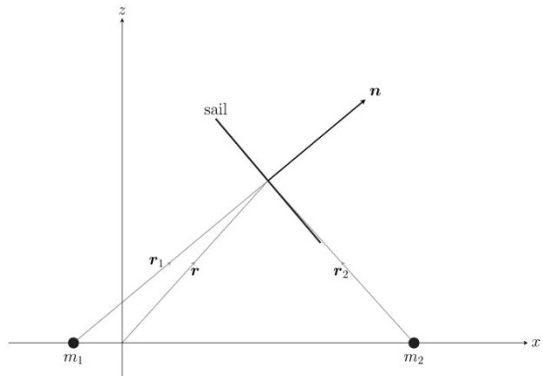

Fig. 1. The solar sail CRTBP, shown in the *x*-*z* plane.

III. Numerical Continuation

One-parameter families of periodic orbits can be continued using boundary value techniques as implemented in the package AUTO [5]. Natural families in a conservative system can be continued through use of an 'unfolding parameter' λ which introduces artificial dissipation into the system [6, 7, 8, 9]. The equations of motion of the system are then given by

$$\ddot{\boldsymbol{r}} + 2\boldsymbol{\omega} \times \dot{\boldsymbol{r}} = \nabla V + \lambda\, \dot{\boldsymbol{r}}.$$

Families are continued in the unfolding parameter, but periodic solutions will always have $\lambda = 0$ to numerical precision. Justification of this approach and its implementation in AUTO can be found in [4, 6, 7, 8, 9], where it is used to follow families in the classical CRTBP as well as detect branch points and continue these in a system parameter. Alternatively, the equations of motion can be reformulated to explicitly include the energy in the equations of motion through the addition of a term of the form

$$\nabla h(\boldsymbol{r}, \mu, \beta)^T (h(\boldsymbol{r}, \mu, \beta) - h_0)$$

where h is the energy, which takes the constant value h_0 along a trajectory. This method permits folds in the energy level to be detected and continued in the system parameter h_0.

Preliminary work has found that the numerical continuation of families of periodic orbits in a reversible system can be implemented in AUTO in a similar way to the unfolding method used for the conservative system.

IV. The Radial Case

The first case investigated is the conservative system with the sail's normal aligned with the Sun-line i.e. $\boldsymbol{n} = \hat{\boldsymbol{r}}_1$. In this modified version of the CRTBP the L_1 Lagrangian equilibrium point remains on the x-axis and moves closer to the Sun as the sail's lightness number increases. This system has been investigated by numerous authors, for example the planar Lyapunov family, or L1 following the notation of [4], and the Halo family, or H1, associated with the L_1 point are known to exist in this case [10, 11, 12, 13]. In particular, [12] found a significant change in the shape of H1 occurs for values of β around 0.04 to 0.05.

We extend on previous results by continuing the L_1 Halo family H1 out to large amplitudes for a wide range of β. Our aim is to provide a full picture of the system's evolution and as such we consider values of the lightness number up to about 0.5, although we recognize that these are not realistic for current solar sail technology.

In the classical case ($\beta = 0$) the H1 family branches from L1 in a pitchfork bifurcation to a north and south branch, symmetric about the x-y plane [4, 10]. We adopt the notation $\mathrm{B}_{\mathrm{L1}}^{\mathrm{H1}}$ for this branch point between families, were in general the lower label indicates the family with the higher symmetry. As the two branches of H1 are identical we will concentrate on the North branch. This family ends in a collision with m_2. At higher mass ratios the collision does not occur and the family connects to a planar family of retrograde circular orbits about both masses, called C2 by [4]. This family bifurcating from C2 still exists in the classical Earth-Sun case, and also ends in a collision with m_2 as would be expected. At higher values of β we find that the increasing amplitudes and changing position of the family means that the collision disappears. Thus we follow H1 from both the L1 and C2 branch points. A bifurcation diagram for the classical case is shown in the first panel of Fig. 2.

As mentioned above, [12] found a marked change in H1 for values of β greater than about 0.04. We also observe this, but find it is due to the appearance of an additional branch point in the family at a critical value of the lightness parameter $\beta_1 \approx 0.0387$. As $\beta \to \beta_1$ the family starts to fold back on itself down to the ecliptic plane. At $\beta = \beta_1$ the family intersects the plane and a branch point appears to a planar family of orbits about m_2, as shown in panel 2 of Fig. 2. This planar family is often referred to in the classical case as the retrograde satellite family and corresponds to Strömgren's family *f* [14, 15], and hence we will label it RS. In the classical case this family is found to contain one branch point to a non-planar family we will call HR, as also shown in panel 1 of Fig. 2.

As β increases above β_1 this branching orbit bifurcates into two and gradually moves apart, essentially splitting the Halo family in half. This is shown in panel 3 of Fig. 2. The second half still ends in collision at this point, but as β increases to about 0.16 this disappears and it reconnects to the C2 half of the family. We call the first 'new' family, the one from the L1 branch point to the first RS branch point, H1B and the second from the other RS branch point to the C2 branch point H1C. These are labeled in Fig. 2.

For completeness we follow these families to higher values of β. Here we find another critical value $\beta_2 \approx 0.2894$ at which the reverse happens: the H1B branch point in RS moves towards and annihilates with the HR branch point (panel 4 of Fig. 2), and the H1B and HR families merge to become a family we designate H1R (panel 5 of Fig. 2). We note that the additional branch points in RS are a result of two folds in β in the locus of the original HR family branch point. In fact as $\beta \to 1$ the branch points in the RS and C2 families merge, as shown in Fig. 3.

The linear stability along the families is determined by the Floquet multipliers (see for example [16]), which are provided by AUTO. As the system is Hamiltonian the multipliers are always reciprocal pairs, and two of the six are unity as they represent perturbations along the periodic orbit. Information about the linear stability of a periodic orbit is therefore determined by the remaining four multipliers. [19] and [12] define order-0 instability as the case with all multipliers on the unit circle, order-1 as one pair only on the unit circle and one pair on the real axis, and order-2 as no multipliers on the unit circle. Generically, changes in the stability can occur at branch points and folds (a pair of multipliers collide at +1), period doubling bifurcations (a pair of multipliers collide at -1), and Krein collisions (two pairs of multipliers collide simultaneously on the unit circle, or for an inverse Krein collision, on the real axis).

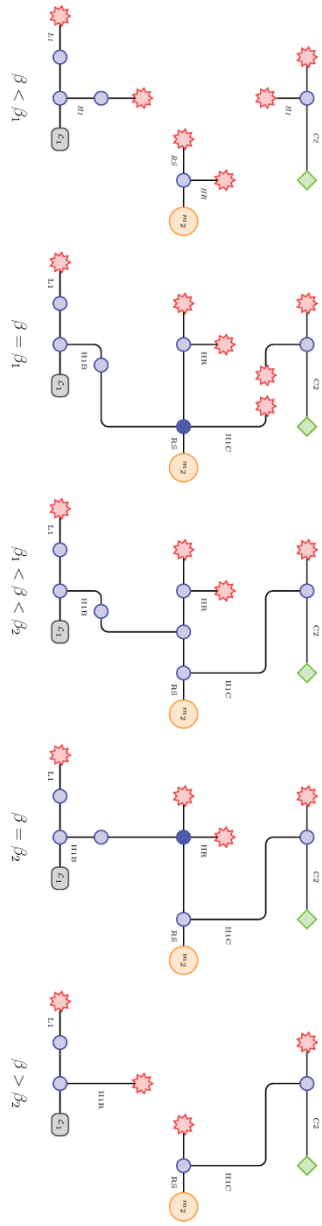

Fig. 2. Schematic bifurcation diagrams of H1 and related families for increasing values of β. Blue circles represent branch points and red stars collisions. The L_1 equilibrium point is shown as a grey rectangle and the secondary mass as a yellow circle. The green diamond indicates that the C2 family appears to continue out to infinity. The darker blue circles represent the two special cases where two branch points in the RS family either appear or collide.

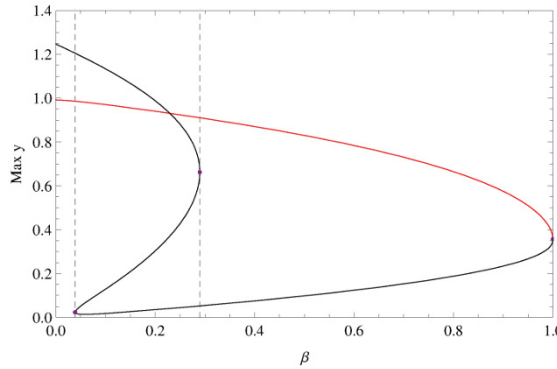

Fig. 3. The evolution of the branch points on the C2 and RS families in β. The C2 branch point is shown in red, the RS branch point in black. The C2 and RS branch points merge at $\beta = 1$. Folds in β are marked as a purple dot. Gray dashed lines mark the region in β for which three branch points exist along the RS family. This region occurs between $\beta_1 \approx 0.0387$ and $\beta_2 \approx 0.2894$.

All these can be detected and continued in AUTO, with the exception of Krein collisions which can be located through examination of the Floquet multipliers. Using these methods we investigate how the linear stability of each family changes as β increases. Fig. 4 shows schematically this stability for the H1, H1B, H1C, HR and H1R families for the entire range of β considered.

For $\beta = 0$ the branch of H1 from L1 is well known to have a small region of order-0 instability defined by a fold and period doubling bifurcation [17], as shown on the left-side of Fig. 4. At small values of β the fold disappears, as does the order-0 region. However, another order-0 region appears, defined by a branch point to an asymmetric family called W5 by [4] and a Krein collision. (This region exists for higher mass ratios in the classical case but is lost in the collision with m_2 here.) Although it appears fairly large on the diagrams, the region is in fact a fairly small portion of each family. As β increases further this region is split by the appearance of two folds. As β approaches the critical value β_1 it becomes part of the H1C family. However, near β_1 a new order-0 region appears in-between a period doubling bifurcation and fold and this continues into H1B. As β approaches 0.041 and 0.045 respectively the fold and period doubling bifurcations disappear and the majority of the region is order-0, defined by the W5 branch point and the branch point to the RS family. This is the large region of order-0 instability seen by [12] at $\beta = 0.05$.

The HR family appears to have order-0 instability for its entirety, and this persists as it merges with the stable part of H1B. These orbits are all large amplitude, and are in marked contrast to orbits obtainable in the classical CRTBP. Examples of the H1, H1B, H1C and H1R families are shown in Fig. 5 to 8, and in each case the order-0 instability portion of the family has been marked. Note that the families are shown on different scales.

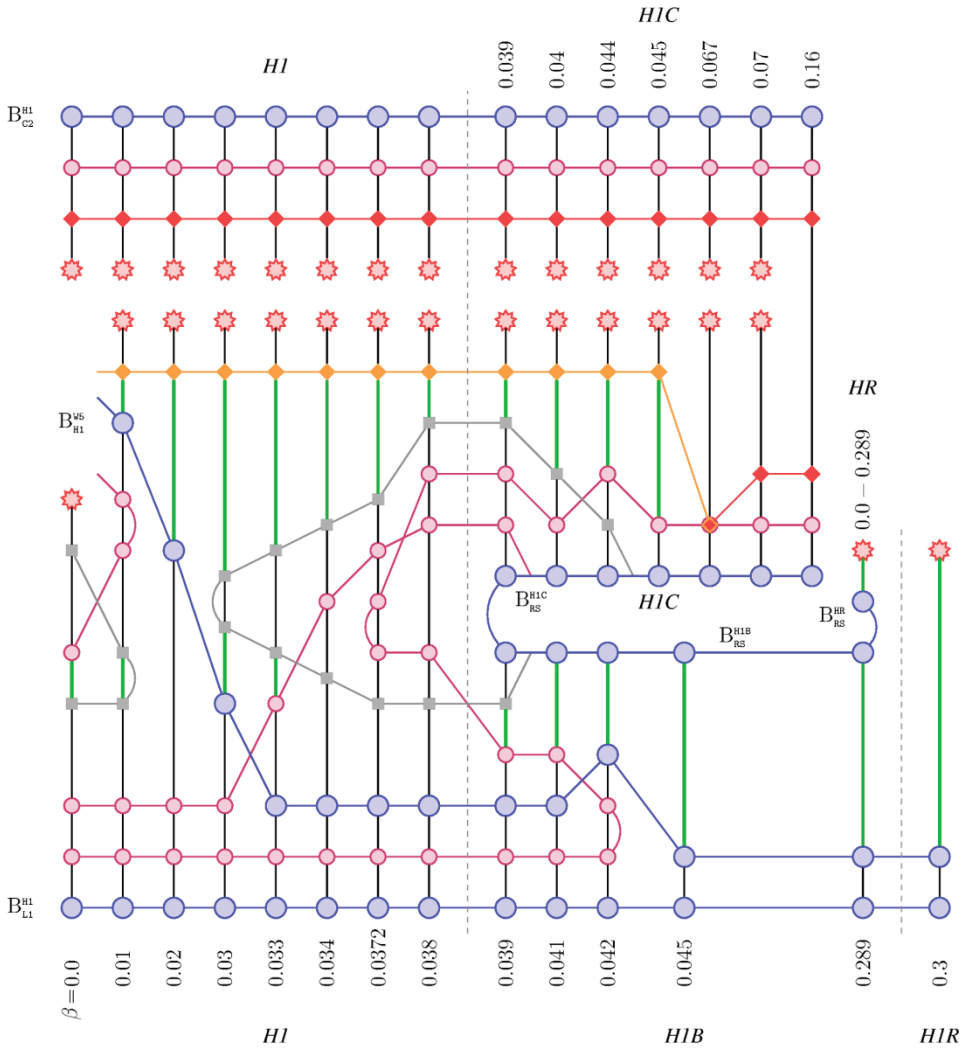

Fig. 4. Stability of H1 and associated families. Vertical lines represent families, and β increases left to right as labeled. Blue circles: branch points to other families, purple circles: period doubling bifurcations, gray squares: folds, orange diamonds: Krein collisions, red diamonds: inverse Krein collisions, red stars: collisions. The thick green line marks the portion of each family that has order-0 instability. The H1 family always starts from the L1 branch point with order-1 instability, and the linear stability of the rest of the family can be deduced from the diagram. The gray dashed lines indicate the points at which the H1 family splits in half or merges with another family. Branch points, period doubling bifurcations and folds have been continued in AUTO and the lines joining these points reflects this. The Krein collisions have been located through examination of each family's Floquet multipliers.

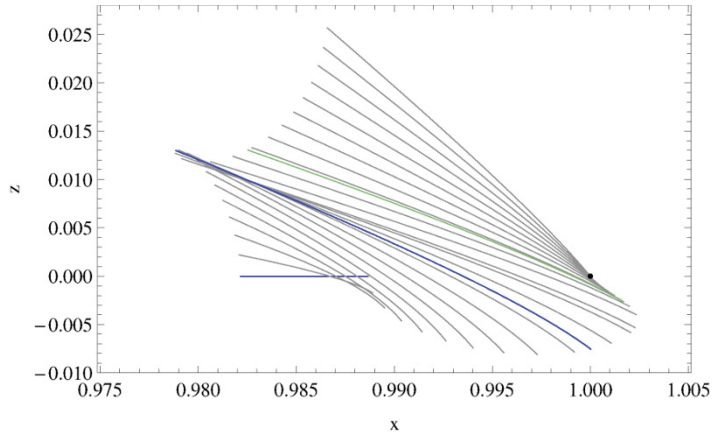

Fig. 5. The H1 family for $\beta = 0.03$, shown in the *x*-*z* plane. Order-0 instability orbits are shown in green, others in gray. The branching orbits to L1 and W5 are shown in blue, and the position of the Earth marked as a black dot.

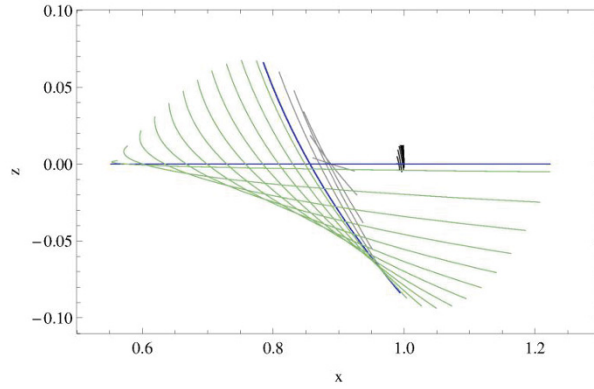

Fig. 6. The H1B family for $\beta = 0.289$, shown in the *x*-*z* plane. Order-0 instability orbits are shown in green, others in gray. The classical H1 family is shown in black for comparison. The branching orbits to L1 and W5 are shown in blue.

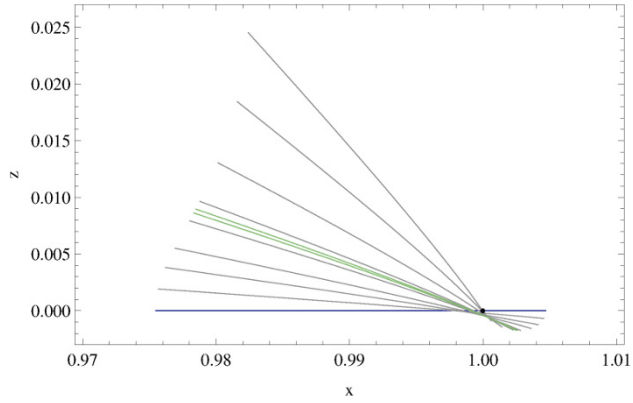

Fig. 7. The H1C family for $\beta = 0.04$, shown in the *x*-*z* plane. Order-0 instability orbits are shown in green, others in gray. The branching orbit to RS is shown in blue, and the position of the Earth marked as a black dot.

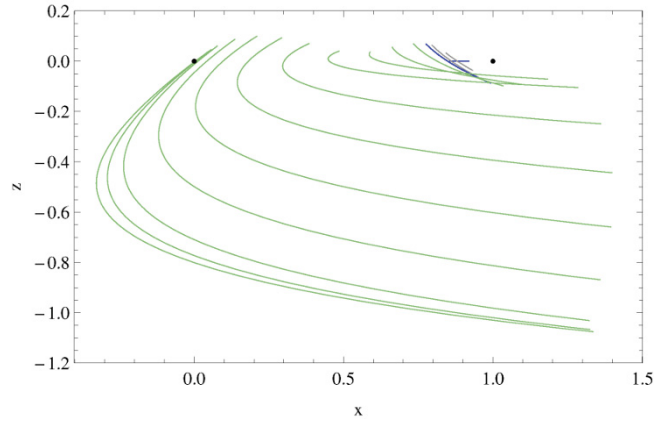

Fig. 8. The H1R family for $\beta = 0.3$, shown in the *x*-*z* plane. Order-0 instability orbits are shown in green, others in gray. The branching orbits to L1 and W5 are shown in blue, and the positions of the Earth and Sun marked as black dots.

V. The Non-Radial Case

The second case we look at is a sail orientated at a constant angle γ to the x-axis, i.e. $\boldsymbol{n} = (\cos\gamma, 0, \sin\gamma)^T$. As mentioned this system is not Hamiltonian, but is reversible, so one-parameter families of periodic orbits exist for fixed values of γ and β. This has previously been considered by [18] and [10]. [18] look at families near L_1 continued in γ, suitable as pole sitter orbits. [10] look at one-parameter families for $\beta = 0.051689$ and show how the L1 to H1 pitchfork bifurcation is broken and the L1 and H1 families merge as the sail angle changes.

In general, five equilibria exist in this system for any fixed values of γ and β, corresponding to the Lagrangian points in the classical case [1, 10, 18]. However, for values of β greater than about 0.15 there is a fold in the curve of equilibria continued from L_1 in γ. That is, there is a small range of angles where three equilibria exist near L_1 instead of one. It can be shown that this coincides with a change in linear stability of one point from center-center-saddle to center-saddle-saddle.

The reversible version of the Lyapunov center theorem [2, 3] implies two families emanate from the points that are center-center-saddle (corresponding to L1 and the vertical family V1 in the classical CRTBP), and one from the center-saddle-saddle point (corresponding to the L1 family). These three points are shown in Fig. 9. We label the center-center-saddle points as L_1^l and L_1^u for the lower and upper point respectively, and the middle center-saddle-saddle point as L_1^m.

Preliminary work has shown that the family emanating from the L_1^m point connects to the lower of the other points, L_1^l. The other family from L_1^l and the two from L_1^u continue out to large amplitudes and are terminated by collisions. These families are also shown in Fig. 9. At large amplitudes the 'vertical' family is similar to large amplitude vertical family orbits in the classical case. However, in contrast to the classical case, some possess order-0 instability.

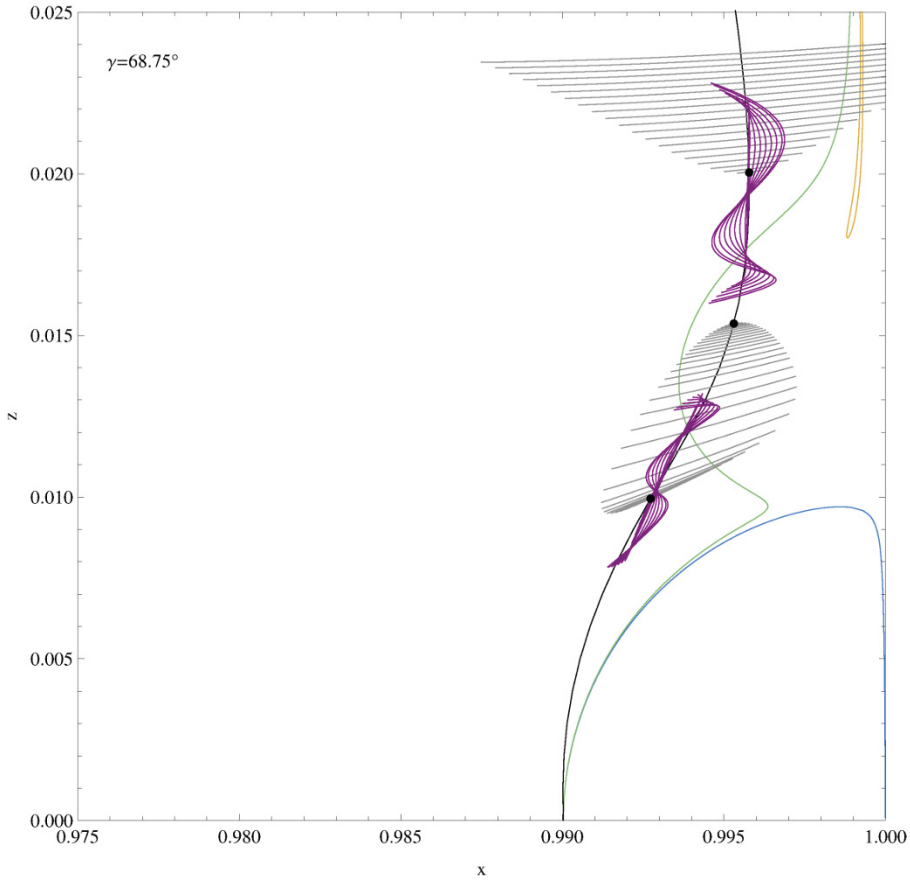

Fig. 9. The families of periodic orbits associated with the three L_1 equilibrium points for $\beta = 0.2$ and $\gamma = 68.75^{\circ}$, shown in the *x*-*z* plane. The equilibria L_1^l, L_1^m and L_1^u are shown as black points, the 'L1' families in gray and the 'V1' families in purple. Note that the families continue out to larger amplitudes than shown here. The black curve is the locus of L_1 in γ for this value of β. The green line marks the location of the fold in γ (for all β) that results in the bifurcation of L_1 into three. The region marked in blue indicates an inaccessible region for L_1, and the region marked in orange a region where the linear stability of L_1^m changes form center-saddle-saddle to center-focus-focus.

VI. Conclusion

Numerical continuation techniques such as those implemented in AUTO provide a means of obtaining a broad overview of periodic orbits obtainable by solar sails, as well as the connections between them and their linear stability.

For a sail orientated perpendicular to the Sun-line the Halo family undergoes significant evolution as the sail's lightness number increases. A fold in the locus of branch point in the retrograde satellite family results in the appearance of two new families of periodic orbits. Even at relatively low lightness numbers these families have fairly large amplitude orbits with order-0 linear instability. Preliminary investigation for a sail orientated instead relative to the Sun-Earth line has shown complex changes occur near the Earth to the L_1 equilibrium point and associated families.

The appearance of large amplitude order-0 instability orbits is a significant difference between solar sails and the classical CRTBP. This provides new opportunities for mission design.

Acknowledgments

This work was funded by the University of Portsmouth's Faculty of Technology.

References

[1] McInnes, C. R., *Solar sailing*, Springer-Praxis, Chichester, UK, 1999

[2] Devaney, R. L., "Reversible Diffeomorphisms and Flows", *Transactions of the American Mathematical Society*, Vol. 218, 1976, pp. 89-113

[3] Sevryuk, M.B., *Reversible Systems*, Lecture Notes in Mathematics, Springer-Verlag, New York, 1986, Chap. 6

[4] Doedel, E. J. et al., "Elemental Periodic Orbits associated with the Libration Points in the Circular Restricted 3-Body Problem", *International Journal of Bifurcation and Chaos*, Vol. 17, No. 8, 2007, pp. 2625-2677
doi: 10.1142/S0218127407018671

[5] Doedel, E. J., Keller, H. B., and Kernévez, J. P., "Numerical analysis and control of bifurcation problems I: bifurcation in finite dimension", *International Journal of Bifurcation and Chaos*, Vol. 1, No. 3, 1991, pp. 493-520
doi: 10.1142/S0218127491000397

[6] Doedel, E. J. et al., "Continuation of periodic solutions in conservative systems with application to the 3-body problem", *International Journal of Bifurcation and Chaos*, Vol. 13, No. 6, 2003, pp. 1353-1381
doi: 10.1142/S0218127403007291

[7] Doedel, E. J., Govaerts, W., Kuznetsov, Y. A., and Dhooge, A., "Numerical continuation of branch points of equilibria and periodic orbits", *International Journal of Bifurcation and Chaos*, Vol. 15, No. 3, 2005, pp. 841-860
doi: 10.1142/S0218127405012491

[8] Calleja, R. C., Doedel, E. J., Humphries, A. R., Lemus-Rodríguez, A., and Oldeman, E. B., "Boundary-value problem formulations for computing invariant manifolds and connecting orbits in the circular restricted three body problem", *Celestial Mechanics and Dynamical Astronomy*, Vol. 114, No. 1-2, 2012, pp. 77-106
doi: 10.1007/s10569-012-9434-y

[9] Munõz-Almaraz, F. J., Freire, E., Galán, J., Doedel, E., and Vanderbauwhede, A., "Continuation of periodic orbits in conservative and Hamiltonian systems", *Physica D Nonlinear Phenomena*, Vol. 181, No. 1-2, 2003, pp. 1-38
doi: 10.1016/S0167-2789(03)00097-6

[10] Farrés, A., and Jorba, À., "Periodic and quasi-periodic motions of a solar sail close to SL1 in the Earth–Sun system", *Celestial Mechanics and Dynamical Astronomy*, Vol. 107, No. 1-2, 2010, pp. 233-253
doi: 10.1007/s10569-010-9268-4

[11] Farrés, A., and Jorba, À., "Dynamics of a solar sail near a Halo orbit", *Acta Astronautica*, Vol. 67, No. 7-8, 2010, pp. 979-990
doi: 10.1016/j.actaastro.2010.05.022

[12] McInnes, A., "Strategies for solar sail mission design in the circular restricted three-body problem", M.S. Dissertation, School of Aeronautics and Astronautics, Purdue University, West Lafayette, IN, 2000

[13] Baoyin, H., and McInnes, C. R., "Solar Sail Halo Orbits at the Sun–Earth Artificial L1 Point", *Celestial Mechanics and Dynamical Astronomy*, Vol. 94, No. 2, 2006, pp. 155-171
doi: 10.1007/s10569-005-4626-3

[14] Hénon, M. "Numerical exploration of the restricted problem, V", *Astronomy and Astrophysics*, Vol. 1, Feb. 1969, pp. 223-238

[15] Strömgren, E., "Connaissance actuelle des orbites dans le problème des trois corps", *Bulletin Astronomique*, Vol. 9, No. 2, 1935, pp. 87-130

[16] Howell, K.C., and Campbell, E.T., "Three-dimensional periodic solutions that bifurcate from Halo families in the circular restricted three-body problem", *Spaceflight Mechanics 1999*, AAS 99-161, AAS, San Diego, CA, 1999, pp. 891-910

[17] Howell, K. C., "Three-Dimensional Periodic Halo Orbits", *Celestial Mechanics*, Vol. 32, No. 1, 1984, pp. 53-71
doi: 10.1007/BF01358403

[18] Waters, T. and McInnes, C.R., "Periodic Orbits Above the Ecliptic in the Solar-Sail Restricted Three-Body Problem", *Journal of Guidance, Control, and Dynamics*, Vol. 30, No. 3, 2007, pp. 687-693
doi: 10.2514/1.26232